

BiDense: Binarization for Dense Prediction

Rui Yin¹ Haotong Qin²

Yong Guo⁵ Jianjun Zhu¹

¹Hanglok-Tech ²ETH Zürich

⁴The Chinese University of Hong Kong

Yulun Zhang³

Wenbo Li⁴

Cheng Wang¹

Biao Jia^{1*}

³Shanghai Jiao Tong University

⁵South China University of Technology

Abstract

Dense prediction is a critical task in computer vision. However, previous methods often require extensive computational resources, which hinders their real-world application. In this paper, we propose BiDense, a generalized binary neural network (BNN) designed for efficient and accurate dense prediction tasks. BiDense incorporates two key techniques: the Distribution-adaptive Binarizer (DAB) and the Channel-adaptive Full-precision Bypass (CFB). The DAB adaptively calculates thresholds and scaling factors for binarization, effectively retaining more information within BNNs. Meanwhile, the CFB facilitates full-precision bypassing for binary convolutional layers undergoing various channel size transformations, which enhances the propagation of real-valued signals and minimizes information loss. By leveraging these techniques, BiDense preserves more real-valued information, enabling more accurate and detailed dense predictions in BNNs. Extensive experiments demonstrate that our framework achieves performance levels comparable to full-precision models while significantly reducing memory usage and computational costs. Project code: <https://github.com/frickyinn/BiDense>

1. Introduction

Dense prediction involves estimating target results for every pixel in an image, including classification tasks (e.g., semantic segmentation), regression tasks (e.g., monocular depth estimation), etc. Traditionally, neural networks designed for dense prediction follow a UNet-like architecture [44], which comprises an encoder and a decoder. Existing methods utilize convolutional neural networks (CNNs) or transformers, employing more parameters and computational operations for more accurate and detailed estimations. However, the increasing demand for computational resources creates a significant barrier to real-world applications, particularly on resource-constrained edge devices.

To compress and accelerate neural networks, many

*corresponding author

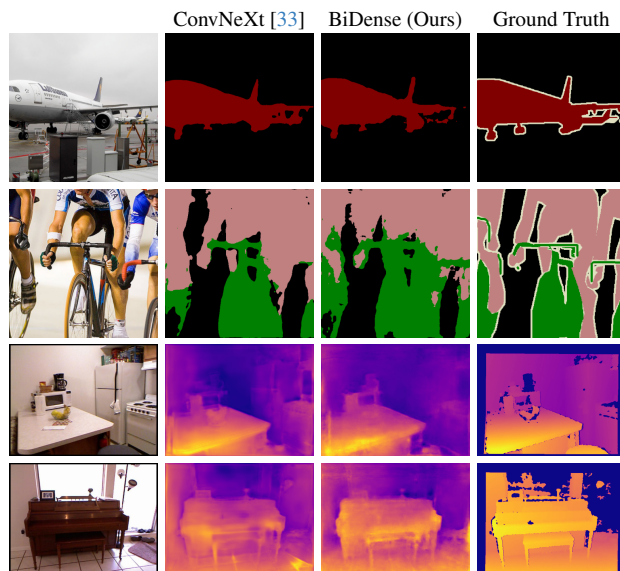


Figure 1. **BiDense** approaches the performance of full-precision 32-bit networks in dense prediction tasks while significantly reducing memory and computational costs.

methods have been proposed [20, 21, 28, 29, 37, 45, 49, 52, 61]. Among these, model quantization [9, 23] stands out for its ability to compress the weights and activations of networks into low-bit representations. As the most extreme form, model binarization restricts all variables to binary values, resulting in binary neural networks (BNNs). By using only 1-bit representations, BNNs achieve a memory compression ratio of up to $32\times$ and a computational reduction of $58\times$ compared to full-precision 32-bit networks. Although model binarization offers substantial resource savings, it often leads to severe performance degradation. As the real-valued variables are binarized, BNNs lose full-precision information, causing drops in accuracy. To mitigate this issue, various methods [3, 19, 30, 34, 42, 50] have been proposed to retain real-valued information during the binarization process. These methods introduce a limited number of full-precision learnable parameters to incorporate binarized variables with real-valued information. However,

since the parameters are fixed after the training stage, they only achieve optimal solutions on the training set. Consequently, they may exhibit inferior performance when faced with unseen cases or fluctuating outlier inputs.

Although some BNNs [66, 67] have focused on resource-intensive dense prediction tasks, they primarily target semantic segmentation and enhancing representation capability. However, the critical challenge for generalized pixel-level estimation is minimizing information loss and effectively incorporating fine-grained features in BNNs to yield more detailed and accurate results. Previous work [3] has proposed specialized binary convolutional layers that allow for full-precision bypasses when the input and output channels mismatch, propagating real-valued fine-grained signals. Yet, it is only applicable when the channel size is reduced by half or increased by double, ineffective in many other situations. Therefore, there is an urgent need to develop generalized techniques that facilitate real-valued skip connections across all channel transformations, thereby minimizing information loss.

To address the aforementioned challenges, we propose a **Binarization** framework for generalized **Dense** prediction tasks (**BiDense**). BiDense incorporates two techniques: the Distribution-adaptive Binarizer (DAB) and the Channel-adaptive Full-precision Bypass (CFB). The DAB leverages the mean and mean absolute deviation (MAD) of full-precision inputs to dynamically determine the binarization thresholds and scaling factors, which captures the information from the distributions of real-valued variables, allowing it to adapt to unseen cases and preserve more messages. Meanwhile, the CFB introduces minimal operations to construct full-precision bypasses for various channel size transformations, thereby minimizing real-valued information loss in binarized dense prediction networks. By integrating these two techniques, BiDense outperforms all previous BNNs and closely approaches the performance of full-precision methods in dense prediction tasks of semantic segmentation and monocular depth estimation, with a minimal increase in parameters and operations. Our contributions can be summarized as follows:

- We propose BiDense, a generalized binarization framework for efficient dense prediction. To the best of our knowledge, this is the first work to apply binarization to the monocular depth estimation task.
- We propose the Distribution-adaptive Binarizer (DAB), which adaptively binarizes activations according to the distribution of real-valued variable inputs, preserving full-precision information.
- We propose the Channel-adaptive Full-precision Bypass (CFB), allowing full-precision skip connections for various channel size transformations in CNNs, thereby minimizing real-valued information loss.
- We evaluate BiDense in dense prediction tasks of seman-

tic segmentation and monocular depth estimation, and show that our framework outperforms SOTA BNNs and achieves performance comparable to full-precision networks while requiring lower computational resources.

2. Related Work

2.1. Dense Prediction

Dense prediction tasks involve pixel-level estimation in images, including semantic segmentation [5, 7, 8, 55, 56, 63], monocular depth estimation [2, 24, 27, 41, 50, 58], key-point detection [11, 17, 43, 51, 59, 64], etc. Neural networks designed for dense prediction typically consist of an encoder and a decoder. The encoder downsamples images to extract high-level semantic information, while the decoder upsamples features and integrates fine-grained details for the final prediction. Fully convolutional methods [4, 15, 24, 27, 35, 50, 55, 63] employ established CNN models [18, 22, 33, 57] as backbones. In contrast, recent frameworks [2, 6, 8, 25, 41, 48, 56, 58] have begun to leverage advanced attention-based models [1, 12, 31, 32, 38, 53] as encoders to further enhance accuracy. While these methods have led to increasingly satisfactory performance, they often require extensive computational resources for precise estimations, which can be challenging for mobile devices. As a remedy, we propose model binarization for dense prediction, significantly reducing memory and computational costs while preserving accuracy to the greatest extent.

2.2. Binary Neural Networks

As the most extreme form of model quantization, model binarization requires neural networks to constrain both weights and activations to either $+1$ or -1 [9, 23]. This approach replaces floating-point operations with bitwise operations and full-precision parameters with 1-bit parameters, significantly accelerating inference and reducing memory usage. However, the binarization process eliminates full-precision information, leading to a substantial drop in accuracy. To address this issue, several methods [3, 19, 30, 34, 39, 42, 50] have been proposed to retain more real-valued information during binarization, thereby improving the performance of BNNs. For instance, ReActNet [30] shifts activations using learned parameters to achieve better binarization distributions; BiT [34] incorporates scaling factors for binary variables; and BiSRNet [3] redistributes activations using learnable linear functions. Although these methods have shown improvements, they are not adaptive to unseen input distributions, which may result in suboptimal performance. Furthermore, while previous BNNs have excelled in low-level vision tasks [3, 26, 54, 62] and simple high-level tasks such as image classification and object detection [19, 30, 34, 39, 50], only a few [66, 67] have focused on the more resource-consuming dense prediction. In response, we propose BiDense to facilitate adaptive retention

of real-valued information, enhancing the accuracy and generalization of dense prediction BNNs.

3. Methods

In this section, we first provide a brief overview of previous binarization methods. Building on existing methods, we then introduce **BiDense**, a **B**inary neural network designed for **D**ense prediction tasks. BiDense incorporates two techniques: the *Distribution-adaptive Binarizer* (DAB) and the *Channel-adaptive Full-precision Bypass* (CFB), which aim to adaptively facilitate the retention and propagation of real-valued, fine-grained information, thereby enhancing performance in dense prediction tasks. Finally, we will elaborate on the implementation details. An overview of the BiDense architecture is summarized in Fig. 2.

3.1. Preliminaries

BNNs are required to constrain both the weights and the activations to either $+1$ or -1 [9, 23]. To achieve this, the sign function is typically used to binarize real-valued variables, resulting in the binarized values \mathbf{B}_x :

$$\mathbf{B}_x = \text{Sign}(x) = \begin{cases} +1 & \text{if } x \geq 0 \\ -1 & \text{otherwise,} \end{cases} \quad (1)$$

where x denotes the full-precision parameters, which include both weights and activations. According to [39], the information entropy of \mathbf{B}_x can be expressed as:

$$\mathcal{H}(\mathbf{B}_x) = -p \ln(p) - (1-p) \ln(1-p), \quad (2)$$

where p is the probability of the value being $+1$, with $p \in (0, 1)$. The entropy of the binary weights or activations serves as a measure of the information richness of the variables. To retain more information, it is optimal for p to equal 0.5 and maximize the entropy, resulting in an even distribution of the binarized values. Ideally, this implies that the optimal binarization threshold corresponds to the median of the real-valued inputs. However, obtaining the median through comparisons can be excessively resource-intensive for BNNs. Thus, IR-Net [39] proposes setting the threshold for the weights to the mean of the full-precision variables. And ReActNet [30] learns the thresholds β as parameters for binarizing the activations:

$$\mathbf{B}_x = \text{Sign}(x - \beta). \quad (3)$$

While learnable parameters can achieve optimal threshold values and maximize information entropy across the entire training set, their fixed nature after training may result in suboptimal solutions in localized contexts or when processing inputs from diverse distributions [19]. As illustrated in Fig. 3, fixed learned thresholds can lead to information loss when applied to unseen data, as indicated by a decrease in entropy. To address the distribution variations and retain more information, we propose two techniques aimed at

adaptively preserving real-valued signals based on the inputs, thereby facilitating more accurate dense predictions.

3.2. Distribution-adaptive Binarizer

Real-valued variables exhibit varying distributions across different image inputs. As shown in Fig. 3, binarizing activations with fixed thresholds can result in fluctuations in information richness after binarization when the input distributions vary. To this end, we propose a dynamic approach for determining the binarization thresholds β , which adaptively redistributes and binarizes real-valued activations according to the input distributions:

$$\mathbf{B}_x = \text{Sign}(x - \beta(x)), \quad (4)$$

$$\beta(x) = k \cdot \bar{x} + b, \quad (5)$$

where k, b are learnable parameters, and \bar{x} denotes the mean of the real-valued variables x . Inspired by [39], we compute our thresholds using the mean to effectively capture the information from input distributions. b learns the average baseline across the entire dataset, akin to [30]. Meanwhile, k quantifies the influence rate of the current inputs, thereby balancing the threshold between global and localized distributions. As indicated in Fig. 3 by information entropy, adaptively determining thresholds effectively enhances information richness after binarization in BiDense.

Following [34], we incorporate a scaling factor $\alpha \in \mathbb{R}_+$ into the binarization function for activations. Bit [34] learns the scale α and threshold β as trainable parameters:

$$\mathbf{B}_x = \alpha \cdot \text{Sign}(x - \beta). \quad (6)$$

Nonetheless, α in Eq. (6) remains fixed after training, preventing it from dynamically recovering the scaling information from the original full-precision values. Therefore, we propose an approach to adaptively obtain α based on the original distributions of the real-valued data. One potential solution involves calculating α by minimizing the l_2 error:

$$\alpha^* = \arg \min_{\alpha \in \mathbb{R}_+} \|\mathbf{x} - \alpha \mathbf{B}_x\|^2 = \frac{\|\mathbf{x}\|_{l1}}{n_x}, \quad (7)$$

where n_x is the number of elements in \mathbf{x} . Essentially, α^* preserves the mean absolute deviation (MAD) of the variables before and after binarization. However, setting the scales of binarized activations to MAD may lead to significant numeric fluctuations in 1-bit variables. Therefore, we introduce a learnable parameter that allows us to control the impact, and the full version of DAB is presented as:

$$\mathbf{x}_s = \mathbf{x} - \beta(\mathbf{x}), \quad (8)$$

$$\mathbf{B}_x = \alpha(\mathbf{x}_s) \cdot \text{Sign}(\mathbf{x}_s), \quad (9)$$

$$\alpha(\mathbf{x}_s) = \exp\left(a \cdot \left(\frac{\|\mathbf{x}_s\|_{l1}}{n_{\mathbf{x}_s}} - 1\right)\right), \quad (10)$$

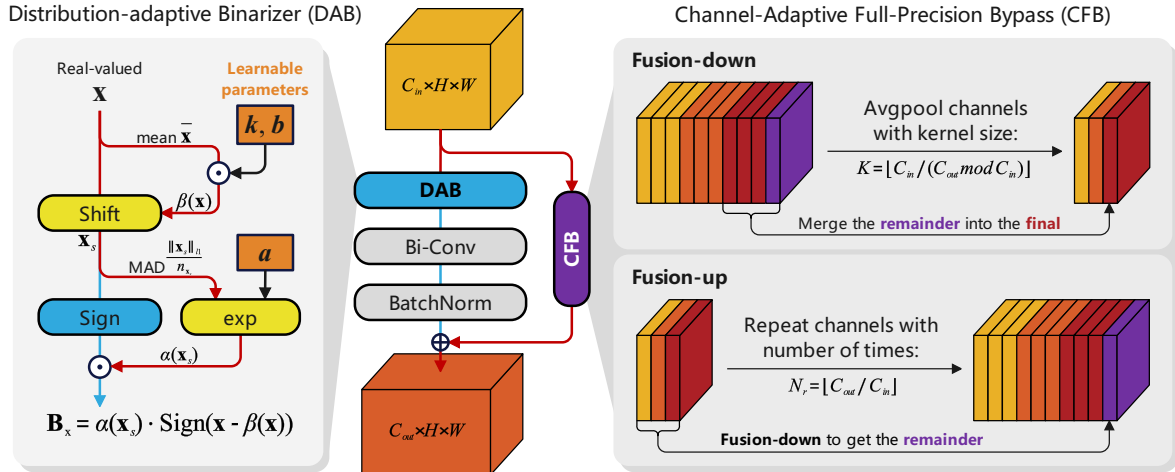


Figure 2. **Overview of a BiDense convolutional layer.** The BiDense layer integrates two techniques: **1) The Distribution-adaptive Binarizer (DAB)** adaptively binarizes activations based on input distributions, allowing it to retain more real-valued information. **2) The Channel-Adaptive Full-precision Bypass (CFB)** employs fusion-down and fusion-up to dynamically adjust the channel size of full-precision features, ensuring they align with the varying shapes of binary convolutional outputs while introducing minimal operations, which facilitates the propagation of real-valued and fine-grained information. **Bi-Conv** represents binary convolution. The **red arrow** ↓ indicates the flow of full-precision information, while the **blue arrow** ↓ denotes the flow of the binarized signal.

Real-valued	BNN [23]	ReActNet [30]	BiDense (Ours)
$\mathcal{H}(\mathbf{B}_{\mathbf{x}}) \rightarrow$	0.481	0.481	0.498
$\mathcal{H}(\mathbf{B}_{\mathbf{x}}) \rightarrow$	0.517	0.540	0.541
$\mathcal{H}(\mathbf{B}_{\mathbf{x}}) \rightarrow$	0.590	0.580	0.607

Figure 3. **Average channel-wise information entropy and feature visualization** of activations before and after the first binarization in networks on the ADE20K [65] validation set. The feature visualization is represented by averaging the activations. As indicated by information entropy, the fixed thresholds in BNN and ReActNet can result in suboptimal binarization and information loss, whereas BiDense retains more information by employing adaptive thresholds in the Distribution-adaptive Binarizer (DAB).

where a is a layer-wise learnable parameter, \mathbf{x}_s denotes variables shifted by the binarization threshold, and $n_{\mathbf{x}_s}$ is the number of elements in \mathbf{x}_s . The parameter α in DAB is dynamically derived based on the MAD of the redistributed real-valued activations. The exponential function \exp en-

sures that α remains greater than 0, while also approximating a linear behavior as input x approaches 1:

$$\lim_{x \rightarrow 1} \exp(a(x - 1)) \approx ax. \quad (11)$$

This linearity preserves the original proportional relationship of the scales. As the influence rate of inputs, a controls the suppression or amplification of the original scaling information. When a is initialized as 0, α can be calculated with an initial value of 1 during the training stage, thereby gradually improving performance from the baseline. DAB binarizes real-valued variables adaptively based on the distribution characteristics of the mean and MAD, enabling enhanced information retention for unseen inputs.

3.3. Channel-adaptive Full-precision Bypass

Neural networks for dense prediction tasks typically consist of an encoder and a decoder to enable pixel-level classification or regression. Both stages incorporate multiple downsampling or upsampling modules, leading to feature channel size reductions or increases. The transformations in channel sizes cause input and output dimension mismatches, obstructing full-precision skip connections, and leading to real-valued information loss and significant drops in prediction performance. To facilitate full-precision bypassing across various channel size transformations for both downsampling and upsampling modules, we propose the Channel-adaptive Full-precision Bypass (CFB).

As shown in Fig. 2, we propose two straightforward techniques: fusion-down and fusion-up, which adaptively transform the channel size of full-precision features, retaining and aggregating real-valued information with minimal ad-

ditional floating point operations. For fusion-down, we apply 1D adaptive average pooling along the channel dimension to reduce the channel size. Different from standard practice, for there is no spatial relationship across channels, we set the kernel size and stride equal to avoid redundant calculations in overlaps. The remainder input channels are merged into the final target channel. In fusion-up, we utilize repetition to increase the channel sizes and employ the fusion-down operation to obtain the remainder target channels and integrate previous messages. Specifically, given a full-precision input $\mathbf{x}_{in} \in \mathbb{R}^{C_{in} \times H \times W}$, where C_{in} , H , W denote the input channel size, height, and width respectively, along with the target channel size C_{out} , the number of times to repeat each channel can be calculated as follows:

$$N_r = \lfloor C_{out}/C_{in} \rfloor. \quad (12)$$

After performing the repetition, the kernel size and stride for average pooling can be determined by:

$$K = \lfloor C_{in}/(C_{out} \bmod C_{in}) \rfloor, \quad (13)$$

and the last $K + (C_{in} \bmod K)$ channels are merged together for pooling. The output of pooling operations is then concatenated with the results from the repetition, if applicable, allowing for adaptive transformations of channel size. By performing the adaptive channel size transformations, the CFB facilitates the propagation of real-valued signals, retaining fine-grained, full-precision information. Meanwhile, binary convolution focuses on learning the residuals, thereby maximizing the information utilization rate.

3.4. Implementation Details

We build the BiDense convolutional layer based on the ReActNet [30] convolutional layer, employing the same techniques for sign approximation functions and scaled binary weights. As depicted in Fig. 2, Batch normalization is utilized within each BiDense layer to normalize the output of binary convolutions, effectively aligning the distributions of these outputs with the real-valued variables from the CFB. To ensure minimal loss of real-valued information, we apply full-precision bypasses across all binarization modules. We leverage the AdamW [36] optimizer along with the OneCycle [47] learning rate scheduler to train our framework on a device with four RTX 3090 GPUs.

4. Experiments

In this section, we first evaluate BiDense on two dense prediction tasks: semantic estimation and monocular depth estimation. Then, we conduct ablation studies and present visualization results to further validate its effectiveness.

Baselines: For the full-precision 32-bit (FP32) baseline, we select ConvNeXt-Tiny [33] as the backbone encoder and UPerNet [55] as the decoder. The classification and regression head are derived from DPT [41]. Building upon this

Method	Bit	Params (K)	OPs (G)	pixAcc (%)	mIoU (%)
ConvNeXt* [33]	32	40,020	288.36	79.48	40.96
ConvNeXt [33]	32	40,023	288.37	70.81	20.39
BNN [23]	1	1,470	4.84	61.69	8.68
ReActNet [30]	1	1,531	4.98	62.77	9.22
AdaBin [50]	1	1,484	5.24	59.47	7.16
BiSRNet [3]	1	1,639	5.07	62.85	9.74
BiDense (Ours)	1	1,626	5.37	67.25	18.75

Table 1. **Semantic segmentation results on the ADE20K [65] validation set.** BiDense outperforms other BNNs in accuracy while maintaining a limited increase in parameters and OPs, approaching the performance of FP32 baselines.

FP32 baseline, we establish 1-bit baselines using previous advanced BNN methods, as well as BiDense with our proposed techniques. For a fair comparison, we provide results from two versions of FP32 baselines: one with pretrained weights on ImageNet [10] for fine-tuning, referred to as ConvNeXt*, and another initialized with random weights for only training on the target datasets, referred to as ConvNeXt. To adapt ConvNeXt for binarization, we modify the network by adding batch normalization after each convolutional layer to mitigate numeric instability caused by consecutive binary operations. This adjustment may lead to a slight increase in parameters and computational operations.

Evaluation Protocols: For each task, we report the accuracy and error metrics following previous work to evaluate and compare the effectiveness. We also provide the number of parameters (Params) and computational operations (OPs). In line with [23], the OPs for BNNs is calculated as $OPs^b = OPs^f/64$, where OPs^f denotes the full-precision operations. Similarly, the parameters of BNN is computed as $Params^b = Params^f/32$, where $Params^f$ indicates the full-precision parameters. The total computational and memory costs of a model can be computed as $OPs = OPs^b + OPs^f$ and $Params = Params^b + Params^f$.

4.1. Semantic Segmentation

We evaluate BiDense using semantic segmentation, which is a pixel-level classification task.

Setup: Following [41], we train and compare multiple methods on ADE20K [65] and PASCAL VOC 2012 [14] training and validation sets, as their test sets are not publicly available. We preprocess the images following [15], setting the input image size to 480×480 pixels for ADE20K and 500×375 pixels for PASCAL VOC during both training and inference. The batch size is set to 32, and the maximum learning rate of the scheduler is configured to 1×10^{-4} . We train the models for 50 epochs on ADE20K and 200 epochs on PASCAL VOC, utilizing the standard cross-entropy loss function. Evaluation metrics, including pixel accuracy (pix-Acc) and mean Intersection-over-Union (mIoU), are computed following the guidelines from [41].

Results: As shown in Tab. 1, BiDense outperforms other

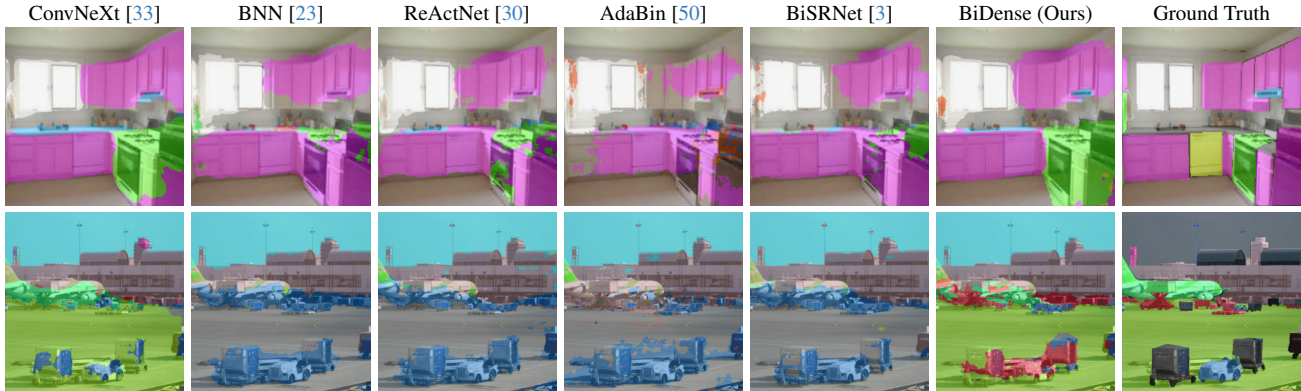


Figure 4. **Qualitative Results of semantic segmentation on the ADE20K [65] validation set.** BiDense preserves full-precision semantic information, yielding more fine-grained and accurate segmentation than previous BNNs.

Method	Bit	Topology	pixAcc (%)	mIoU (%)
ConvNeXt* [33]	32		98.58	99.72
ConvNeXt [33]	32	ConvNeXt-Tiny, UPerNet	96.02	84.6
LQ-Net [60]	3		-	62.5
Group-Net [67]	1	ResNet-18, FCN-32s	-	65.1
CBNN [66]	1		-	66.5
LQ-Net [60]	3		-	70.4
Group-Net [67]	1	ResNet-34, FCN-32s	-	72.8
LQ-Net [60]	3		-	70.7
Group-Net [67]	1	ResNet-50, FCN-32s	-	71.0
BNN [23]	1		83.57	40.1
ReActNet [30]	1		83.38	42.1
AdaBin [50]	1	ConvNeXt-Tiny, UPerNet	78.27	25.2
BiSRNet [3]	1		86.30	47.5
BiDense (Ours)	1		92.73	75.2

Table 2. **Semantic segmentation results on the PASCAL VOC 2012 [14] validation set.** BiDense outperforms prior quantized models, delivering finer-grained results.

BNN baselines on ADE20K in terms of pixAcc and mIoU, while maintaining a comparable number of parameters and OPs. Compared to FP32 baselines, BiDense has 4.06% of the parameters and 1.86% of the OPs, with only 3.56% and 1.64% reductions of pixAcc and mIoU, respectively. Moreover, when compared to previous BNNs, BiDense achieves remarkable improvements in terms of pixAcc and mIoU by 4.40% and 9.01%, respectively, with only a limited increase in parameters and OPs. Tab. 2 further demonstrates the superior performance of BiDense on the PASCAL VOC datasets. BiDense outperforms all prior quantized models and approaches the FP32 baseline in semantic segmentation, highlighting the effectiveness of our framework in preserving semantic content and real-valued information. The qualitative results of semantic segmentation are also demonstrated in Fig. 4, where BiDense displays highly fine-grained and accurate results compared to other baselines.

4.2. Monocular Depth Estimation

We also evaluate BiDense for monocular depth estimation, a pixel-level regression task in dense prediction.

Setup: Following [41], we utilize the NYUv2 [46] and KITTI [16] depth datasets to assess our method. The images are preprocessed according to [27], with input image sizes of 416×544 for NYUv2 and 352×704 for KITTI, in both training and inference stages. For NYUv2, we use a batch size of 32 and set the maximum learning rate of the scheduler to 6×10^{-5} . For KITTI, the batch size is 64, and the maximum learning rate is 1×10^{-4} . We employ the standard Silog loss function [13, 27] to train all the methods. Metrics are reported following the evaluation procedure outlined in [40]. For δ_1 , δ_2 , and δ_3 , higher values indicate better performance, while for the error metrics AbsRel, RMSE, log10, and RMSE log, lower values are preferred.

Results: Tab. 3 presents the quantitative results of monocular depth estimation. Again, BiDense outperforms all previous BNNs in the task. On the KITTI dataset, our framework closely approaches the FP32 baseline, demonstrating comparable performance, while on the NYUv2 dataset, BiDense achieves even higher accuracy and lower errors across all metrics compared to the FP32 network. We attribute this superior performance to the effectiveness of the CFB in retaining real-valued information and detailed content. The skip connections and aggregation within the CFB minimize information loss, allowing the binary convolutional layers to effectively capture deep features. The qualitative results of depth estimation are illustrated in Fig. 5, where BiDense delivers accurate depth predictions with competitive precision relative to the FP32 method.

4.3. Ablation Study

We conduct ablation studies to evaluate the efficacy of the DAB and CFB using the ADE20K [65] datasets. Specifically, we set BiDense as the baseline and compare it to various variants established by removing or substituting specific techniques with other methods. Tab. 4 presents the detailed results of our ablation studies. First, we demonstrate the effectiveness of the complete set of techniques: **1) Removing the DAB** disables the adaptive binarization to differ-

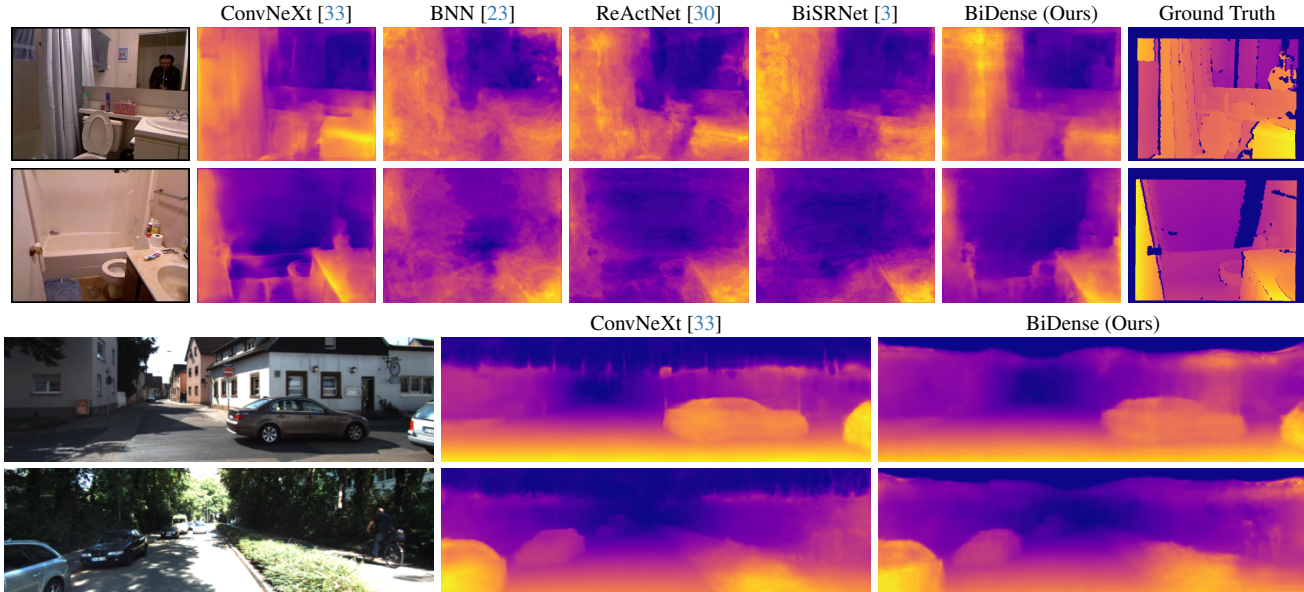


Figure 5. **Qualitative results of monocular depth estimation results on the NYUv2 [46] and KITTI [16] depth datasets.** BiDense retains real-valued information, resulting in more accurate performance and finer-grained depth predictions compared to previous BNNs.

Method	Bit	NYUv2 [46]						KITTI [16]				RMSE	log10
		δ_1	δ_2	δ_3	AbsRel	RMSE	log10	δ_1	δ_2	δ_3	AbsRel		
ConvNeXt* [33]	32	0.871	0.979	0.996	0.117	0.407	0.050	0.958	0.996	0.999	0.065	2.416	0.094
ConvNeXt [33]	32	0.695	0.916	0.975	0.201	0.641	0.081	0.902	0.980	0.996	0.092	3.429	0.137
BNN [23]	1	0.644	0.887	0.966	0.223	0.712	0.091	0.889	0.976	0.993	0.102	3.610	0.150
ReActNet [30]	1	0.664	0.898	0.969	0.215	0.686	0.088	0.893	0.976	0.993	0.099	3.449	0.146
AdaBin [50]	1	0.537	0.826	0.945	0.256	0.851	0.112	0.853	0.962	0.990	0.119	4.016	0.173
BiSRNet [3]	1	0.659	0.897	0.970	0.214	0.682	0.088	0.890	0.976	0.994	0.101	3.567	0.147
BiDense (Ours)	1	0.712	0.921	0.978	0.189	0.610	0.078	0.896	0.979	0.995	0.095	3.389	0.139

Table 3. **Monocular depth estimation results on the NYUv2 [46] and KITTI [16] depth datasets.** Our framework outperforms all previous BNNs on both datasets. With the CFB, BiDense achieves even superior performance than the FP32 baseline on NYUv2.

Method	Params (K)	OPs(G)	pixAcc	mIoU
ConvNeXt [33]	40,023	288.37	70.81	20.39
ReActNet [30]	1,531	4.98	62.77	9.22
BiDense (Full)	1,626	5.37	67.25	18.75
1) w/o DAB	1,484	5.11	66.32	18.10
2) w/o CFB	1,626	5.28	63.20	9.78
3) w/o thresholds β	1,531	5.24	67.04	17.96
4) w/o $k\bar{x}$, $\beta(\mathbf{x}) = b$	1,579	5.31	67.17	18.01
5) w/o b , $\beta(\mathbf{x}) = k\bar{x}$	1,579	5.37	66.72	17.56
6) w/o scaling factors α	1,579	5.24	66.96	18.09
7) set $\alpha(\mathbf{x}_s) = \ \mathbf{x}_s\ _{l1}/n_{\mathbf{x}_s}$	1,579	5.37	49.3	4.97
8) set α as learnable parameters	1,626	5.31	65.14	15.10

Table 4. **Ablation study on the ADE20K [65] datasets.** Our proposed techniques improve the performance of dense predictions.

ent distributions of unseen inputs, which diminishes the information richness of features after binarization in BiDense and reduces estimation accuracy. **2) Removing the CFB** results in a significant accuracy drop, as this eliminates the ability to retain real-valued information for convolutional layers undergoing various channel-size transformations in

dense prediction networks, leading to considerable information loss. Yet, with the DAB, BiDense still outperforms its 1-bit baseline, ReActNet.

Threshold: Then, we examine the roles of the adaptive thresholds $\beta(\mathbf{x})$ in our Distribution-adaptive Binarizer (DAB) by comparing the DAB to previous binarizers and its possible variants: **3) Removing the thresholds β** prevents variable redistribution, which undermines information richness after binarization and results in accuracy drops. **4) Setting β as learnable parameters**, similar to [30], fails to capture information from input distributions, leading to sub-optimal binarization threshold values for unseen inputs. **5) Without b** , setting $\beta(\mathbf{x}) = k\bar{x}$ causes fluctuations in binarization thresholds due to the mean \bar{x} influenced by outliers, resulting in suboptimal values.

Scale: Additionally, we compare the adaptive scaling factors $\alpha(\mathbf{x}_s)$ with other variants to study its role in performance. **6) By removing the scaling factors α** , the network struggles to retain essential real-valued information across different scales, resulting in a drop in accuracy. **7) Setting**

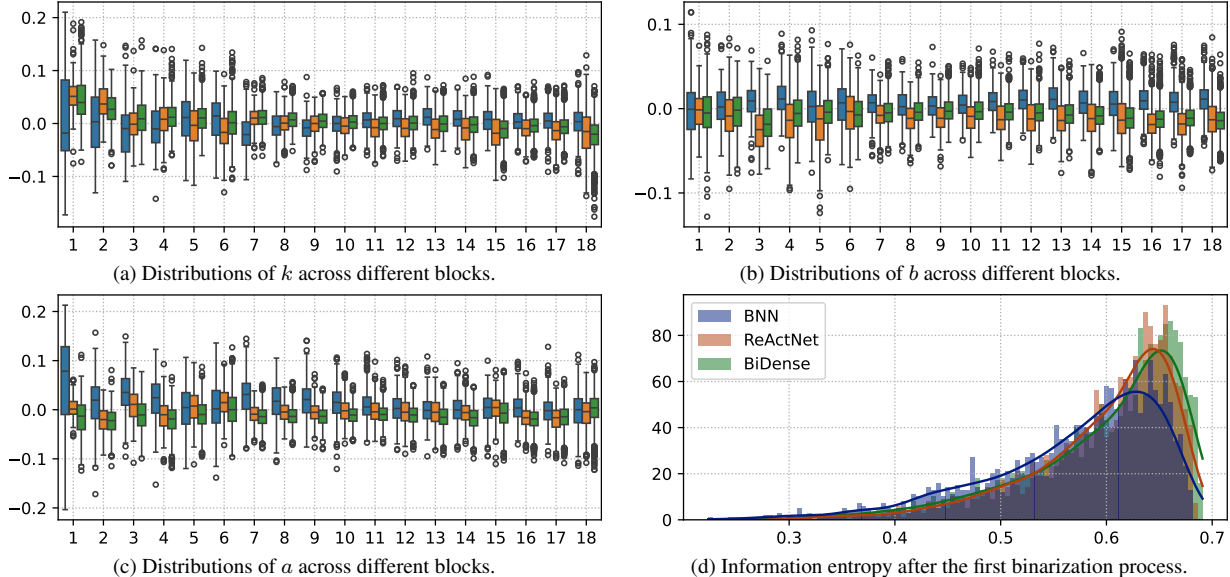


Figure 6. **Statistics of DAB on the ADE20K [65] validation set.** 1) Panels (a), (b), and (c) illustrate the statistics of three learnable parameters, k , b , and a , from three different convolutional modules across the 18 ConvNeXt blocks, ranging from shallow to deep layers. The colors blue, orange, and green represent the three consecutive convolutions within each block. Their distributions exhibit variability and all demonstrate bottleneck shapes throughout the layers. 2) Panel (d) presents the statistics of average channel-wise information entropy after the initial binarization process in the networks for all inputs from the ADE20K validation set. BiDense generally shows higher entropy, indicating a greater average information richness after binarization and retains the most information.

the scales to MAD introduces significant fluctuations as the variables transition from real-valued to 1-bit, complicating the training process and hindering robust performance. 8) **Making α learnable parameters**, similar to [34], leads to accuracy drops on the validation set, because fixed parameters take on suboptimal values for unseen data. The ablation study results validate the effectiveness of our proposed CFB and DAB. By integrating these two techniques, BiDense enables adaptive real-valued information retention, leading to superior overall performance in dense predictions.

4.4. Visualization

In Fig. 6, we visualize the statistics for BiDense, presenting the distributions of the learnable parameters and comparing the information entropy across different methods.

Learnable parameters: First, we report the value distributions of the three learnable parameters, k , b , and a , proposed in our DAB. Given that the ConvNeXt backbone comprises three types of convolutions, each serving a distinct role within a ConvNeXt block, we visualize their parameter statistics separately using three different colors. Fig. 6a, 6b, and 6c illustrate the distributions of these parameters across the 18 blocks in the ConvNeXt backbone, spanning from shallow to deep layers. The distributions exhibit variation across different convolutional modules within the blocks and across different network layers, suggesting that the parameters are optimized for improved binarization at various positions within the network. The distributions of the three parameters across the blocks exhibit a bottleneck shape,

mirroring the overall architecture of the backbone.

Information Entropy: Fig. 6d illustrates the information entropy of the activations after the first binarization process across different binary networks. Overall, the entropy levels of BNN, ReActNet, BiDense increase in that order, indicating a greater richness of information as the methods evolve. With the DAB, BiDense dynamically sets binarization thresholds to accommodate varying input value distributions, thereby enhancing information retention.

5. Conclusion

This paper proposes BiDense, a generalized binarization framework for efficient and accurate dense prediction tasks. BiDense integrates two techniques: the Distribution-adaptive Binarizer (DAB) and the Channel-adaptive Full-Precision Bypass (CFB). To adaptively retain more real-valued information for unseen data, the DAB utilizes the mean and the mean absolute deviation to derive binarization thresholds and scaling factors, which effectively capture real-valued information from input distributions. Meanwhile, to facilitate full-precision bypasses when input and output feature dimension mismatch due to channel transformations in binary convolutional layers, the CFB incorporates minimal operations to adjust the channel size of full-precision features, propagating real-valued signals through various binary modules, thereby minimizing information loss. We demonstrate that BiDense outperforms SOTA BNNs in the dense prediction tasks of semantic segmentation and monocular depth estimation, achieving accuracy comparable to that of full-precision networks while requiring significantly lower computational resources.

References

- [1] Hangbo Bao, Li Dong, Songhao Piao, and Furu Wei. Beit: Bert pre-training of image transformers. *arXiv preprint arXiv:2106.08254*, 2021. 2
- [2] Shariq Farooq Bhat, Reiner Birkel, Diana Wofk, Peter Wonka, and Matthias Müller. Zoedepth: Zero-shot transfer by combining relative and metric depth. *arXiv preprint arXiv:2302.12288*, 2023. 2
- [3] Yuanhao Cai, Yuxin Zheng, Jing Lin, Xin Yuan, Yulun Zhang, and Haoqian Wang. Binarized spectral compressive imaging. In *NeurIPS*, 2024. 1, 2, 5, 6, 7
- [4] Liang-Chieh Chen. Rethinking atrous convolution for semantic image segmentation. *arXiv preprint arXiv:1706.05587*, 2017. 2
- [5] Liang-Chieh Chen, Yukun Zhu, George Papandreou, Florian Schroff, and Hartwig Adam. Encoder-decoder with atrous separable convolution for semantic image segmentation. In *ECCV*, 2018. 2
- [6] Zhe Chen, Yuchen Duan, Wenhai Wang, Junjun He, Tong Lu, Jifeng Dai, and Yu Qiao. Vision transformer adapter for dense predictions. *arXiv preprint arXiv:2205.08534*, 2022. 2
- [7] Bowen Cheng, Alex Schwing, and Alexander Kirillov. Pixel classification is not all you need for semantic segmentation. In *NeurIPS*, 2021. 2
- [8] Bowen Cheng, Ishan Misra, Alexander G Schwing, Alexander Kirillov, and Rohit Girdhar. Masked-attention mask transformer for universal image segmentation. In *CVPR*, 2022. 2
- [9] Matthieu Courbariaux, Yoshua Bengio, and Jean-Pierre David. Binaryconnect: Training deep neural networks with binary weights during propagations. In *NeurIPS*, 2015. 1, 2, 3
- [10] Jia Deng, Wei Dong, Richard Socher, Li-Jia Li, Kai Li, and Li Fei-Fei. Imagenet: A large-scale hierarchical image database. In *CVPR*, 2009. 5
- [11] Daniel DeTone, Tomasz Malisiewicz, and Andrew Rabinovich. Superpoint: Self-supervised interest point detection and description. In *CVPRW*, 2018. 2
- [12] Alexey Dosovitskiy. An image is worth 16x16 words: Transformers for image recognition at scale. *arXiv preprint arXiv:2010.11929*, 2020. 2
- [13] David Eigen, Christian Puhrsch, and Rob Fergus. Depth map prediction from a single image using a multi-scale deep network. In *NeurIPS*, 2014. 6
- [14] Mark Everingham, Luc Van Gool, Christopher KI Williams, John Winn, and Andrew Zisserman. The pascal visual object classes (voc) challenge. In *ICCV*, 2010. 5, 6
- [15] Jun Fu, Jing Liu, Haijie Tian, Yong Li, Yongjun Bao, Zhiwei Fang, and Hanqing Lu. Dual attention network for scene segmentation. In *CVPR*, 2019. 2, 5
- [16] Andreas Geiger, Philip Lenz, and Raquel Urtasun. Are we ready for autonomous driving? the kitti vision benchmark suite. In *CVPR*, 2012. 6, 7
- [17] Pierre Gleize, Weiyao Wang, and Matt Feiszli. Silk: Simple learned keypoints. In *ICCV*, 2023. 2
- [18] Kaiming He, Xiangyu Zhang, Shaoqing Ren, and Jian Sun. Deep residual learning for image recognition. In *CVPR*, 2016. 2
- [19] Yefei He, Zhenyu Lou, Luoming Zhang, Jing Liu, Weijia Wu, Hong Zhou, and Bohan Zhuang. Bivit: Extremely compressed binary vision transformers. In *ICCV*, 2023. 1, 2, 3
- [20] Geoffrey Hinton, Oriol Vinyals, and Jeff Dean. Distilling the knowledge in a neural network. In *NeurIPS*, 2015. 1
- [21] Andrew G Howard, Menglong Zhu, Bo Chen, Dmitry Kalenichenko, Weijun Wang, Tobias Weyand, Marco Andreetto, and Hartwig Adam. Mobilenets: Efficient convolutional neural networks for mobile vision applications. *arXiv preprint arXiv:1704.04861*, 2017. 1
- [22] Gao Huang, Zhuang Liu, Laurens Van Der Maaten, and Kilian Q Weinberger. Densely connected convolutional networks. In *CVPR*, 2017. 2
- [23] Itay Hubara, Matthieu Courbariaux, Daniel Soudry, Ran El-Yaniv, and Yoshua Bengio. Binarized neural networks. In *NeurIPS*, 2016. 1, 2, 3, 4, 5, 6, 7
- [24] Lam Huynh, Phong Nguyen-Ha, Jiri Matas, Esa Rahtu, and Janne Heikkilä. Guiding monocular depth estimation using depth-attention volume. In *ECCV*, 2020. 2
- [25] Jitesh Jain, Jiachen Li, Mang Tik Chiu, Ali Hassani, Nikita Orlov, and Humphrey Shi. Oneformer: One transformer to rule universal image segmentation. In *CVPR*, 2023. 2
- [26] Xinrui Jiang, Nannan Wang, Jingwei Xin, Keyu Li, Xi Yang, and Xinbo Gao. Training binary neural network without batch normalization for image super-resolution. In *AAAI*, 2021. 2
- [27] Jin Han Lee, Myung-Kyu Han, Dong Wook Ko, and Il Hong Suh. From big to small: Multi-scale local planar guidance for monocular depth estimation. *arXiv preprint arXiv:1907.10326*, 2019. 2, 6
- [28] Hao Li, Asim Kadav, Igor Durdanovic, Hanan Samet, and Hans Peter Graf. Pruning filters for efficient convnets. In *ICLR*, 2017. 1
- [29] Zechun Liu, Baoyuan Wu, Wenhan Luo, Xin Yang, Wei Liu, and Kwang-Ting Cheng. Bi-real net: Enhancing the performance of 1-bit cnns with improved representational capability and advanced training algorithm. In *ECCV*, 2018. 1
- [30] Zechun Liu, Zhiqiang Shen, Marios Savvides, and Kwang-Ting Cheng. Reactnet: Towards precise binary neural network with generalized activation functions. In *ECCV*, 2020. 1, 2, 3, 4, 5, 6, 7
- [31] Ze Liu, Yutong Lin, Yue Cao, Han Hu, Yixuan Wei, Zheng Zhang, Stephen Lin, and Baining Guo. Swin transformer: Hierarchical vision transformer using shifted windows. In *ICCV*, 2021. 2
- [32] Ze Liu, Han Hu, Yutong Lin, Zhuliang Yao, Zhenda Xie, Yixuan Wei, Jia Ning, Yue Cao, Zheng Zhang, Li Dong, et al. Swin transformer v2: Scaling up capacity and resolution. In *CVPR*, 2022. 2
- [33] Zhuang Liu, Hanzi Mao, Chao-Yuan Wu, Christoph Feichtenhofer, Trevor Darrell, and Saining Xie. A convnet for the 2020s. In *CVPR*, 2022. 1, 2, 5, 6, 7

- [34] Zechun Liu, Barlas Oguz, Aasish Pappu, Lin Xiao, Scott Yih, Meng Li, Raghuraman Krishnamoorthi, and Yashar Mehdad. Bit: Robustly binarized multi-distilled transformer. In *NeurIPS*, 2022. 1, 2, 3, 8
- [35] Jonathan Long, Evan Shelhamer, and Trevor Darrell. Fully convolutional networks for semantic segmentation. In *CVPR*, 2015. 2
- [36] Ilya Loshchilov and Frank Hutter. Decoupled weight decay regularization. In *ICLR*, 2018. 5
- [37] Ningning Ma, Xiangyu Zhang, Hai-Tao Zheng, and Jian Sun. Shufflenet v2: Practical guidelines for efficient cnn architecture design. In *ECCV*, 2018. 1
- [38] Maxime Oquab, Timothée Darcet, Théo Moutakanni, Huy Vo, Marc Szafraniec, Vasil Khalidov, Pierre Fernandez, Daniel Haziza, Francisco Massa, Alaaeldin El-Nouby, et al. Dinov2: Learning robust visual features without supervision. *arXiv preprint arXiv:2304.07193*, 2023. 2
- [39] Haotong Qin, Ruihao Gong, Xianglong Liu, Mingzhu Shen, Ziran Wei, Fengwei Yu, and Jingkuan Song. Forward and backward information retention for accurate binary neural networks. In *CVPR*, 2020. 2, 3
- [40] René Ranftl, Katrin Lasinger, David Hafner, Konrad Schindler, and Vladlen Koltun. Towards robust monocular depth estimation: Mixing datasets for zero-shot cross-dataset transfer. *IEEE transactions on pattern analysis and machine intelligence*, 2020. 6
- [41] René Ranftl, Alexey Bochkovskiy, and Vladlen Koltun. Vision transformers for dense prediction. In *ICCV*, 2021. 2, 5, 6
- [42] Mohammad Rastegari, Vicente Ordonez, Joseph Redmon, and Ali Farhadi. Xnor-net: Imagenet classification using binary convolutional neural networks. In *ECCV*, 2016. 1, 2
- [43] Jerome Revaud, Cesar De Souza, Martin Humenberger, and Philippe Weinzaepfel. R2d2: Reliable and repeatable detector and descriptor. In *NeurIPS*, 2019. 2
- [44] Olaf Ronneberger, Philipp Fischer, and Thomas Brox. U-net: Convolutional networks for biomedical image segmentation. In *MICCAI*, 2015. 1
- [45] Mark Sandler, Andrew Howard, Menglong Zhu, Andrey Zhmoginov, and Liang-Chieh Chen. Mobilenetv2: Inverted residuals and linear bottlenecks. In *CVPR*, 2018. 1
- [46] Nathan Silberman, Derek Hoiem, Pushmeet Kohli, and Rob Fergus. Indoor segmentation and support inference from rgb-d images. In *ECCV*, 2012. 6, 7
- [47] Leslie N Smith and Nicholay Topin. Super-convergence: Very fast training of neural networks using large learning rates. In *Artificial intelligence and machine learning for multi-domain operations applications*, 2019. 5
- [48] Robin Strudel, Ricardo Garcia, Ivan Laptev, and Cordelia Schmid. Segmenter: Transformer for semantic segmentation. In *ICCV*, 2021. 2
- [49] Vivienne Sze, Yu-Hsin Chen, Tien-Ju Yang, and Joel S Emer. Efficient processing of deep neural networks: A tutorial and survey. *Proceedings of the IEEE*, 2017. 1
- [50] Zhijun Tu, Xinghao Chen, Pengju Ren, and Yunhe Wang. Adabin: Improving binary neural networks with adaptive binary sets. In *ECCV*, 2022. 1, 2, 5, 6, 7
- [51] Michał Tyszkiewicz, Pascal Fua, and Eduard Trulls. Disk: Learning local features with policy gradient. In *NeurIPS*, 2020. 2
- [52] Huan Wang and Yun Fu. Trainability preserving neural pruning. In *ICLR*, 2023. 1
- [53] Wenhui Wang, Hangbo Bao, Li Dong, Johan Bjorck, Zhiliang Peng, Qiang Liu, Kriti Aggarwal, Owais Khan Mohammed, Saksham Singhal, Subhojit Som, et al. Image as a foreign language: Beit pretraining for vision and vision-language tasks. In *CVPR*, 2023. 2
- [54] Bin Xia, Yulun Zhang, Yitong Wang, Yapeng Tian, Wenming Yang, Radu Timofte, and Luc Van Gool. Basic binary convolution unit for binarized image restoration network. In *ICLR*, 2023. 2
- [55] Tete Xiao, Yingcheng Liu, Bolei Zhou, Yuning Jiang, and Jian Sun. Unified perceptual parsing for scene understanding. In *ECCV*, 2018. 2, 5
- [56] Enze Xie, Wenhai Wang, Zhiding Yu, Anima Anandkumar, Jose M Alvarez, and Ping Luo. Segformer: Simple and efficient design for semantic segmentation with transformers. In *NeurIPS*, 2021. 2
- [57] Saining Xie, Ross Girshick, Piotr Dollár, Zhuowen Tu, and Kaiming He. Aggregated residual transformations for deep neural networks. In *CVPR*, 2017. 2
- [58] Lihe Yang, Bingyi Kang, Zilong Huang, Xiaogang Xu, Jiashi Feng, and Hengshuang Zhao. Depth anything: Unleashing the power of large-scale unlabeled data. In *CVPR*, 2024. 2
- [59] Kwang Moo Yi, Eduard Trulls, Vincent Lepetit, and Pascal Fua. Lift: Learned invariant feature transform. In *ECCV*, 2016. 2
- [60] Dongqing Zhang, Jiaolong Yang, Dongqiangzi Ye, and Gang Hua. Lq-nets: Learned quantization for highly accurate and compact deep neural networks. In *ECCV*, 2018. 6
- [61] Xiangyu Zhang, Xinyu Zhou, Mengxiao Lin, and Jian Sun. Shufflenet: An extremely efficient convolutional neural network for mobile devices. In *CVPR*, 2018. 1
- [62] Yulun Zhang, Haotong Qin, Zixiang Zhao, Xianglong Liu, Martin Danelljan, and Fisher Yu. Flexible residual binarization for image super-resolution. In *ICML*, 2024. 2
- [63] Hengshuang Zhao, Jianping Shi, Xiaojuan Qi, Xiaogang Wang, and Jiaya Jia. Pyramid scene parsing network. In *CVPR*, 2017. 2
- [64] Xiaoming Zhao, Xingming Wu, Jinyu Miao, Weihai Chen, Peter CY Chen, and Zhengguo Li. Alike: Accurate and lightweight keypoint detection and descriptor extraction. *IEEE Transactions on Multimedia*, 2022. 2
- [65] Bolei Zhou, Hang Zhao, Xavier Puig, Sanja Fidler, Adela Barriuso, and Antonio Torralba. Scene parsing through ade20k dataset. In *CVPR*, 2017. 4, 5, 6, 7, 8
- [66] Xichuan Zhou, Rui Ding, Yuxiao Wang, Wenjia Wei, and Haijun Liu. Cellular binary neural network for accurate image classification and semantic segmentation. *IEEE Transactions on Multimedia*, 2022. 2, 6
- [67] Bohan Zhuang, Chunhua Shen, Mingkui Tan, Lingqiao Liu, and Ian Reid. Structured binary neural networks for accurate image classification and semantic segmentation. In *CVPR*, 2019. 2, 6